Natalia Konieczna, Janusz Adamiec

Susceptibility of Alloy IN617 to Hot Cracking

Abstract: The article presents results of tests concerning the susceptibility of alloy IN617 to hot cracking. The research-related tests required the inert gas-shielded melting of test alloy sheets using a tungsten electrode in forced strain conditions. The process of melting involved 3 mm and 5 mm thick test sheets. The tests of the welded joints included the macro and microstructural analysis of the molten area, base material and heat affected zone. Results obtained in the DTA differential analysis were used to perform tests using a Gleeble 3800 simulator. In the above-presented manner it was possible to determine the high-temperature brittleness range (HTBR) of alloy IN617 as well as to identify the effect of strains on the development of hot cracks in the Transvarestraint test. The tests were supplemented with the fractographic analysis of the crack area. It was revealed that the hot cracking phenomenon occurred within the high-temperature brittleness range of the alloy and depended on the size of strain as well as on the presence of eutectics formed in the solid-liquid state.

Keywords: metallography, Gleeble, DTA, hot cracking, Inconel 617

DOI: *10.17729/ebis.2018.4/5*

Introduction

Nickel alloys belong to advanced materials which, because of their high-temperature creep resistance and heat resistance are used in the power industry in elements exposed to temperatures exceeding 650°C. One of the nickel alloys enumerated in technical documentation as a material used in stem superheater coil is IN617 [1]. The above-named alloy is subjected to solid solution hardening. Because of alloying agents including chromium, molybdenum and cobalt, alloy IN617 is characterised by good mechanical properties and resistance to oxidation at high temperatures. Due to the formation of hot cracks, IN617 is regarded as hard-to-weld [2]. Hot cracks can be generated in the weld (solidification cracking) or in the heat affected zone (HAZ) (liquation cracking) [3,4].

Previous discussions related to the hot cracking of materials were primarily related to the presence of low-melting eutectics, particularly sulphuric and phosphoric, triggering strains resulting in the racking of welds. Luckily, the development of metallurgy successfully restrained the presence of impurities in the material [4]. Presently, hot cracking-related criteria can be divided into two groups. The first group only includes metallurgical criteria, whereas the second group includes criteria connected with critical stress, strain and strain rate [5]. The above-presented criteria apply to a limited extent as regards advanced materials, including IN617. Previous tests

mgr inż. Natalia Konieczna (MSc Eng.); dr hab. inż. Janusz Adamiec (PhD (DSc) Habilitated Eng.), Professor at Silesian University of Technology, Institute of Materials Engineering, Katowice

confirmed that hot cracks are formed within the high-temperature brittleness range (HTBR). There is a lack of explicit definitions of the high-temperature brittleness range (HTBR) during welding, i.e. the range of temperature where the material is characterised by reduced plasticity and susceptibility to hot cracking [6,7]. According to N.N. Prokhorowa [8] the liquidus temperature should be recognised as the upper limit of the HTBR, whereas the solidus temperature should be recognised as the lower limit of the HTBR. In turn, J.F. Lancaster [9] assumed the existence of a temperature, where crystals become joined forming a coherent, yet not entirely solidified mass characterised by certain strength. Therefore, the HTBR constitutes the difference between the nil strength temperature (NST) during heating and the ductility recovery temperature (DRT) during cooling.

Reference publications do not contain information specifying the reason for hot racking in alloy IN617. Because of this, it is necessary to describe structural phenomena occurring in alloy IN617 within the above-named temperature range. The tests aimed to assess the susceptibility of alloy IN617 to hot cracking and to identify the high-temperature brittleness range, i.e. the temperature range, where the alloy is in the solid-liquid state and is susceptible to hot cracking in welding conditions.

Test Materials and Methodology

The tests involved 1 mm, 3 mm and 5 mm thick sheets made of alloy Inconel 617. The chemical composition of the alloy was verified for conformity with the ASME SB-168:2013 standard [10] and the conformity certificate provided by the manufacturer in relation to each test sheet. The verification was performed using the XRF method and a Niton XL2 machine. An exemplary XRF spectrum related to 3 mm thick alloy Inconel 617 is presented in Figure 1. The percentage content of individual chemical elements is presented in Table 1. The analysis results revealed that the chemical composition of the alloy determined using the XRF method was restricted within the range specified by the above-named ASME standard and was consistent with the conformity certificate.

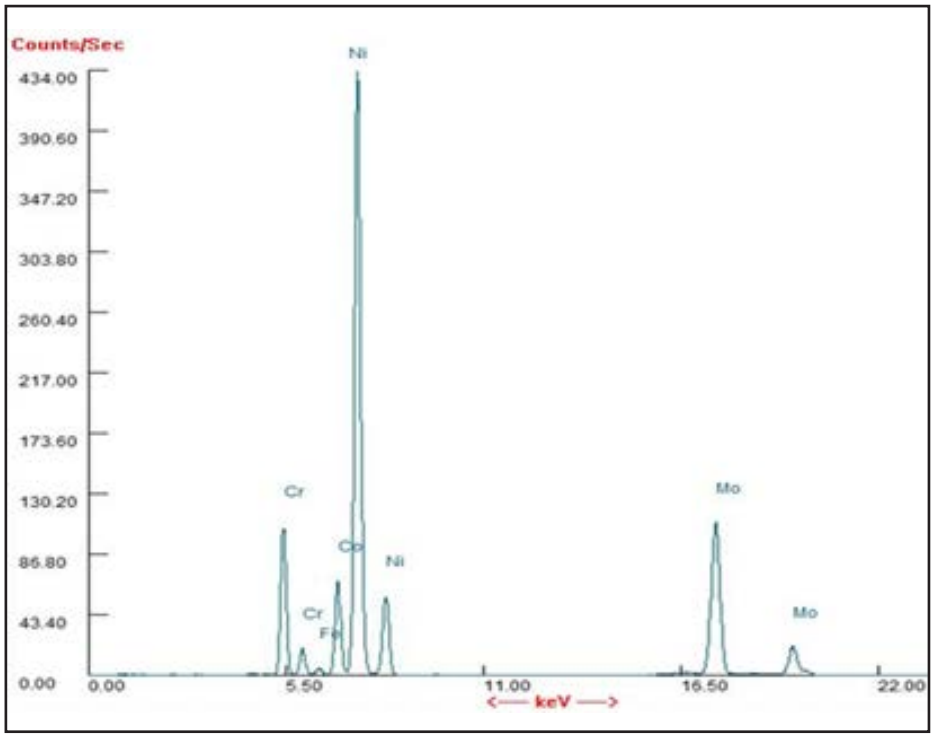

Table 1. Chemical composition of nickel alloy IN617 in relation to 3 mm thick sheet, determined using the XRF method and according to conformity certificate and standard ASME SB-168:2013, % by weight [10]

IN617	Cr	Co	Mo	Al	Fe	Mn	Si	Ti	Cu	S	P	B	C
XRF	19.17	12.11	9.87	-	0.89	-	-	0.28	-	-	-	-	-
Conformity certificate	21.72	11.66	8.74	1.01	1.40	0.07	0.16	0.41	0.18	0.002	0.003	0.001	0.58
ASME SB-168:2013	20-24	10-15	8-10	0.8-1.5	max 3.0	max 1.0	max 1.0	max 0.6	max 0.5	max 0.015	-	max 0.006	0.05-0.15

The identification of characteristic temperatures of the crystallisation of the alloy involved the performance of a differential thermal analysis (DTA). The DTA tests were performed using a SETSYS thermal analyser (Setaram). The DTA involved the use of an "S" type thermocouple (Pt-Rh /Pt-Rh 10%). The specimens were heated up to a temperature of 1500°C at a rate of 10°C/min; the flow rate of argon amounted to 1.35 l/h.

The obtained temperature of solidus and that of liquidus were used in tests performed using a Gleeble 3800 thermomechanical simulator. The tests enabled the determination of the nil strength temperature (NST) and the nil ductility temperature (NDT) as well as the ductility recovery temperature (DRT) during cooling. The results obtained in the DTA were used to determine the high-temperature brittleness range (HTBR), defined as the difference between the nil strength temperature (NST) during heating and the ductility recovery temperature (DRT) during cooling.

To determine the NST it was necessary to weld an S type thermocouple to cylindrical specimens made of alloy IN617 (φ 6 × 90 mm). Afterwards, the specimens were placed in the copper holders of the simulator. The specimen under the minimum initial load, restricted within the range of 0.6kN to 0.7kN, was heated at a rate of 20°C/s up to a temperature of 1200°C and next, at a rate of 1°C/s up to the temperature of rupture. The NST was determined as the mean value of five specimens, at which cracks appeared. In relation to the test alloy the mean NST amounted to 1330°C.

To determine the NDT of alloy IN617 it was necessary to heat the specimens up to a preset temperature within the HTBR, next, hold the specimens at the above-named temperature for 10 s and, finally, extend them at a constant rate of 20 mm/s.

The DRT was determined as the temperature where the area reduction of the specimens was below 5%. The specimens were cooled from a temperature close to the NST to the preset temperature and, next, were extended at a constant rate. Both in the NDT and DRT-related test the adjusted welding rate amounted to 20 mm/s.

The subsequent stage involved the performance of a TIG method-based melting test in forced strain conditions (Transvarestraint test). The Transvarestraint test involves the bending of test sheets/plates on a cylindrical matrix block perpendicularly in relation to the melting direction (Fig. 2).

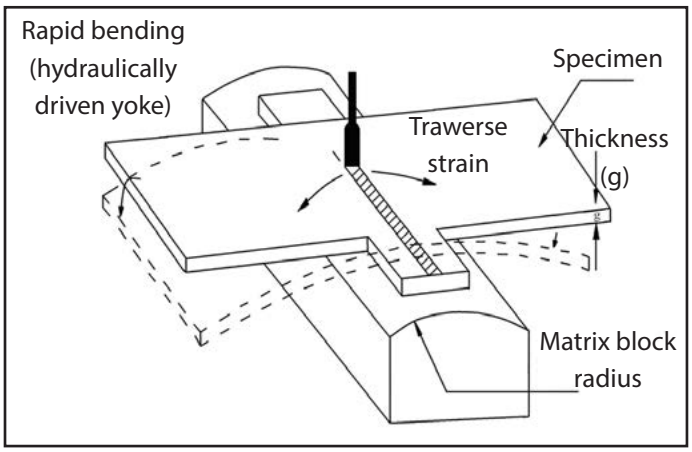

Fig. 2. Schematic Transvarestraint test [11]

Specimens used in metallographic tests were cut out of fusion areas following the Transvarestraint test. To reveal all of the joint zones, the specimens were cut out perpendicularly in relation to the direction of electric arc movement. Metallographic analysis also involved the specimens subjected to the test performed using the Gleeble simulator. The cut-out specimens were subjected to electrochemical etching performed for 15 seconds at a voltage of 6V in Lucas' reagent. The tests involved structural analysis performed using an Olympus SZX 9 stereoscopic microscope (SM). The microstructural observation was performed using an Olympus GX71 light microscope (LM) and a magnification of up to 500x in the bright field. The tests also involved structural analysis performed using a JEOL JCM-6000 Neoscope II and a Hitachi S-3400 scanning electron microscope (SEM). Images were recorded using the secondary electron (SE) technique at a magnification of up to 3000x. The tests were supplemented with the

microanalysis of the chemical composition performed using the EDS method. In the tests particular attention was given to areas where cracks were revealed.

Test Results

Differential thermal analysis (DTA)

The differential thermal analysis (DTA) enabled the identification of characteristic temperatures related to the heating and cooling of alloy IN617 on DTA curves. The temperature of the beginning and that of the end of the transformation were determined using the method involving the intersection of two tangents. The results obtained in the analysis are presented in Table 2. During heating, the crystals of the liquid phase appeared at a temperature of 1343°C (T_{N1}). The initial melting point corresponded to the maximum on the endothermic peak and amounted to 1394°C (T_{Npeak}), whereas the final melting point during heating amounted to 1420°C (T_{N2}). The cooling process was also used to identify characteristic temperatures, i.e. the temperature at which the first crystals of the solid phase were formed (liquidus temperature T_L amounting to 1390°C) and the temperature at which the process of crystallisation finished (solidus temperature T_S amounting to 1279°C). During cooling the temperature of crystallisation amounted to 1380°C (T_{Cpeak}).

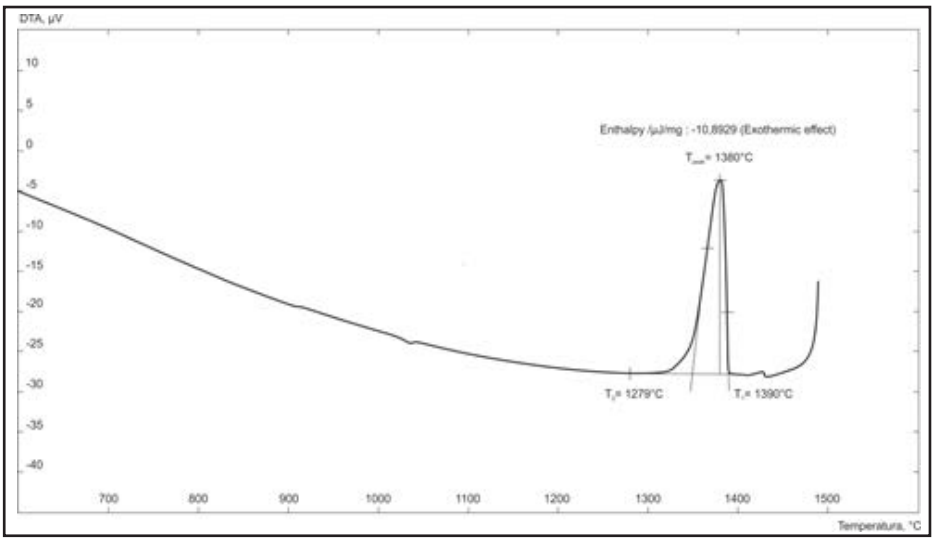

Fig. 3. DTA curve during cooling in relation to IN617

Table 2. Transformation-related characteristic temperatures in relation to alloy IN617

T_{N1}, °C	T_{Npeak}, °C	T_{N2}, °C	T_L, °C	T_{Cpeak},°C	T_S, °C
1343	1394	1420	1390	1380	1279

The tests related to the susceptibility of the welded joints made of alloy IN617 involved the adoption of the solidus temperature and liquidus temperature determined during the cooling related to the weld crystallisation process during the cooling of the joint. An exemplary DTA curve related to the cooling of alloy IN617 is presented in Figure 3.

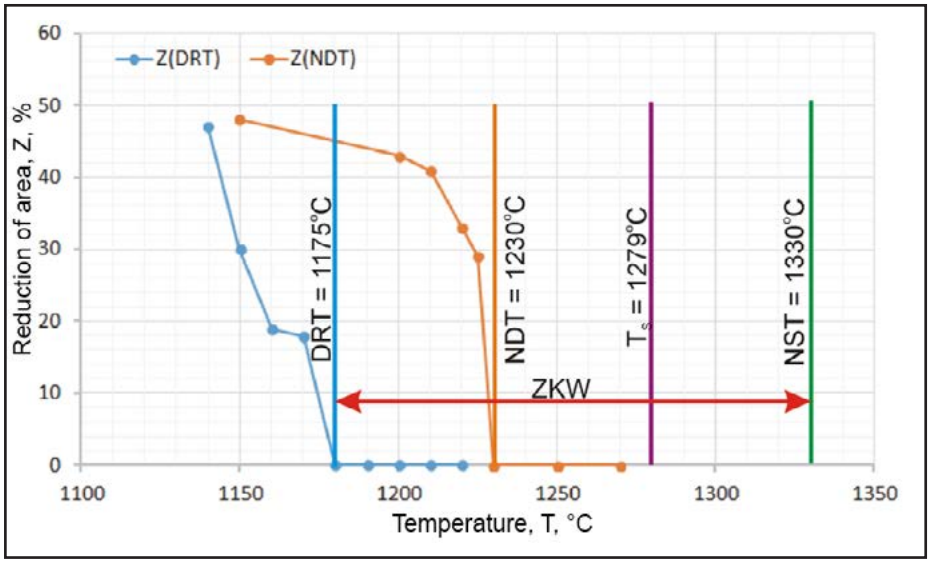

Fig. 4. Elongation of alloy Inconel 617 in the function of temperature during heating (NDT) and during cooling (DRT)

Tests performed using a Gleeble 3800 simulator

The high-temperature brittleness range determined using the Gleeble simulator amounted to 155°C. Area reductions in the specimens in the function of temperature during heating (identification of the NDT) and cooling (identification of the DRT) are presented in Figure 4.

The tests performed using the Gleeble simulator were supplemented with the metallographic analysis of crack areas formed during heating and cooling. An example of a structure following the DRT tests is presented in Figure 5. The tests concerning the structure of nickel alloy IN617 after the DRT tests revealed the mesh of cracks along matrix γ grain boundaries with numerous scrap-induced crack (Fig. 5a).

The loss of the alloy cohesion resulted from the connection of cracks along grain boundaries, which, in turn, led to the formation of the mesh of cracks and its development into the primary crack. The foregoing was confirmed by fractographic tests of the fracture surface. The fracture surface revealed polygonal grains of matrix γ with numerous scrap-induced cracks along grain boundaries (Fig. 5b). It was also possible to observe bridges between individual grains, typical of hot cracking within the high-temperature brittleness range.

Transvarestraint Test

The Transvarestraint test performed in forced strain conditions enabled the determination of the size of strain ε, defined as the proportion of the test sheet thickness to the double curvature radius. The correlation between the size of the strain of the 5 mm thick sheet and the total length of cracks, the number of cracks and the longest crack is presented in Fig. 6.

The analysis of the face of fusion (Fig. 7) led to the conclusion that the lower the bend angle the longer the length of a crack. The tests were

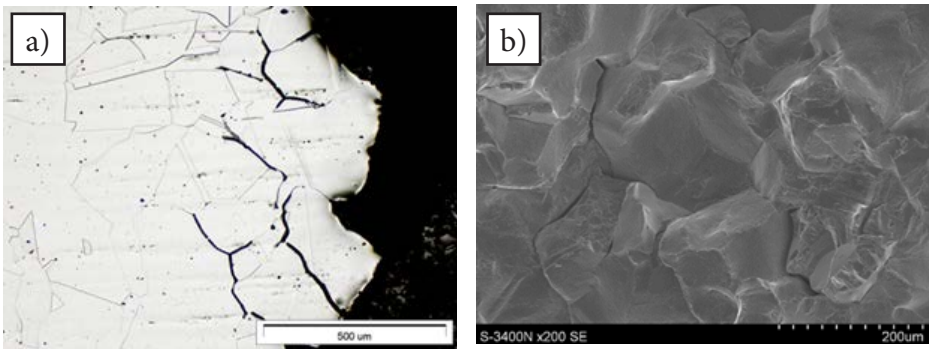

Fig. 5. Structure of the crack area of nickel alloy Inconel 617 after the DRT test: a) microstructure of the area perpendicular to the fracture, local partial melting of the grains of matrix γ (LM) b) fracture surface, visible partial melting of the grains of the matrix with the mesh of intercrystalline scrap-induced cracks and the bridges between the grains (SE)

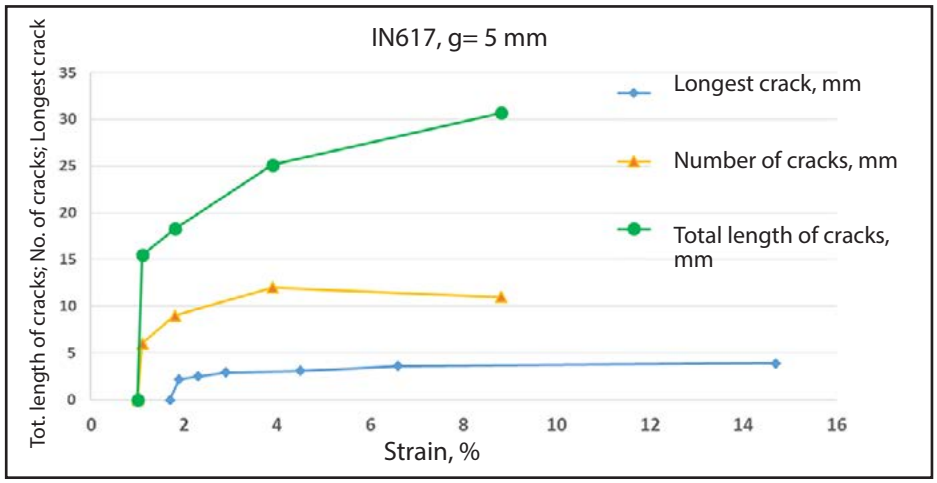

Fig. 6. Correlation between the strain and the length of the longest crack, the number of cracks and the total length of cracks in relation to the 5 mm thick welded joints made of alloy IN617

Fig. 7. Faces of fusion in alloy IN 617 (g=5 mm) with visible cracks (SM): a) bend angle of 38 mm, longest crack of 3.6 mm, b) bend angle of 85 mm., longest crack of 2.9 mm, c) bend angle of 135 mm, longest crack of 2.2 mm

followed by the analysis of the crack area. The area was characterised by the solidified layer of liquid (Fig. 8a), formed in the liquid-solid state of the alloy in the high-temperature brittleness range. The layer was located between the dendrites of the weld. The cracks formed in forced strains were hot cracks, i.e. manifested by ruptured bridges between dendrites. The foregoing was confirmed by observation results concerned with the crack fracture (Fig. 8b).

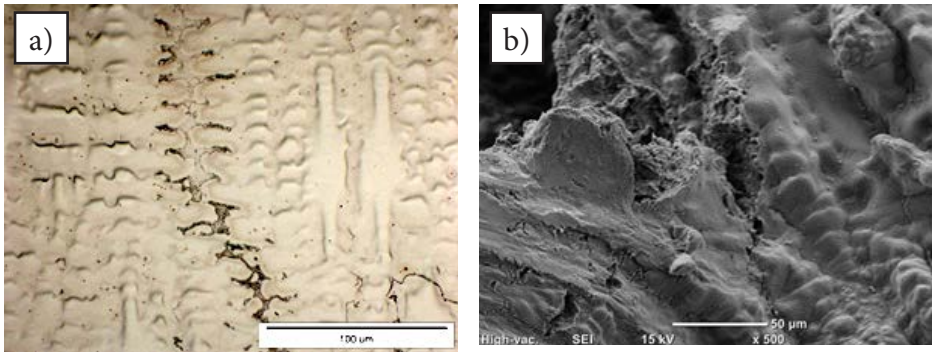

Fig. 8. Structure of alloy IN617 in the crack area: a) solidified layer of the liquid from the HTBR (LM) b) crack surface, visible ruptured bridges between the dendrites (SEM)

Summary

The tests revealed that nickel alloy IN617 crystallised within the temperature range of 1370°C to 1279°C. Based on the foregoing it was ascertained that during the cooling of alloy IN617 the range between the solidus temperature and the liquidus temperature amounted to 111°C. The obtained results enabled the identification of the high-temperature brittleness range extension amounting to 155°C. Within the above-presented temperature range alloy IN 617 was susceptible to hot cracking. The alloy subjected to the tests revealed the presence of hot cracks characterised by ruptured bridges. The primary reason for the hot cracking of alloy IN617 was the partial melting of material grain boundaries and the loss of intercrystalline liquid continuity. An additional factor triggering hot cracking in alloy IN617 was the solidified layer of liquid formed in the liquid-solid state within the high-temperature brittleness range.

Further research related to hot cracking susceptibility will involve the determination of hot cracking indicators such as temperature-related stress intensity and a critical strain rate.

References

[1] Maile M.: *Qualification of Ni-Based Alloys for Advanced Ultra Supercritical Plants.* Procedia Engineering. 2013, 55, pp. 214–220. https://doi.org/10.1016/j.proeng.2013.03.245

[2] Klöwer J., Husemann R. U., Bader M.: *Development of Nickel Alloys Based on Alloy 617 for Components in 700°C Power Plants.* Procedia Engineering. 2013, 55, pp. 226–331. https://doi.org/10.1016/j.proeng.2013.03.247

[3] Bollinghaus T., Herold H., Cross C. E., Lippold J. C: *Hot Cracking Phenomena in Welds II*. Berlin 2008, Springer. http://dx.doi.org/10.1007/978-3-540-78628-3

[4] Tasak E.: *Metalurgia spawania*. Kraków 2008, Wydawnictwo JAK.

[5] Ma L.: I*dentifying and Understanding Environment-Induced Crack Propagation Behavior in Solid Strengthened Ni-Based Superalloys*. 2012, Project No. 09-803. University of Nevada.

[6] DuPont J., Lippold J., Kiser S.: *Welding metallurgy and weldability of nickel-base alloys*. 2009, New York, John Wiley & Sons. http://dx.doi.org/10.1002/9780470500262

[7] Turowska A., Adamiec J.: *Evaluation of high temperature corrosion resistance of finned tubes made of austenitic steel and nickel alloys*. Archives of Metallurgy and Materials, 2016, no. 61 (2), pp. 1089-1093. http://dx.doi.org/10.1515/amm-2016-0183

[8] Prokhorov N.N.: *Russian Castings Production*. 1962, 2, p. 172.

[9] Lancaster J.F.: *The metallurgy of welding, brazing and soldering*. George Allen& Unwin Ltd, London, 1965. http://dx.doi.org/10.1017/s0368393100081864

[10] Asme sb-168:2013: Specification for nickel-chromium-iron alloys (UNS N06600, N06601, N06603, N06690, N06693, N06025, and N06045) and nickel- chromium-cobalt-molybdenum alloy (UNS N06617) plate, sheet and strip.

[11] Adamiec J.: 2010. *Spawalność odlewniczych stopów magnezu*. Gliwice, Wydawnictwo Politechniki Śląskiej.